

Using H α Filaments to Probe AGN Feedback in Galaxy Clusters

YU QIU (邱宇)^{†,1}, TAMARA BOGDANOVIĆ^{‡,1}, YUAN LI,² AND MICHAEL McDONALD³

¹*Center for Relativistic Astrophysics, Georgia Institute of Technology, Atlanta, GA 30332*

²*Department of Astronomy, University of California, Berkeley, CA 94720*

³*Kavli Institute for Astrophysics and Space Research, MIT, Cambridge, MA 02139*

ABSTRACT

Recent observations of giant ellipticals and brightest cluster galaxies (BCGs) provide tentative evidence for a correlation between the luminosity of the H α emitting gas filaments and the strength of feedback associated with the active galactic nucleus (AGN). Motivated by this, we use 3D radiation-hydrodynamic simulations with the code **Enzo** to examine and quantify the relationship between the observable properties of the H α filaments and the kinetic and radiative feedback from supermassive black holes in BCGs. We find that the spatial extent and total mass of the filaments show positive correlations with AGN feedback power and can therefore be used as probes of the AGN activity. We also examine the relationship between the AGN feedback power and velocity dispersion of the H α filaments and find that the kinetic luminosity shows statistically significant correlation with the component of the velocity dispersion along the jet axis but not the components perpendicular to it.

Keywords: galaxies: clusters: general — galaxies: clusters: intracluster medium — hydrodynamics — radiative transfer

1. INTRODUCTION

Observational evidence indicates that feedback from active galactic nuclei (AGNs), powered by accretion onto the supermassive black holes (SMBHs), has a profound impact on their host galaxies and clusters. In cool-core clusters (CCCs), for example, AGN feedback is thought to be the primary mechanism which prevents catastrophic radiative cooling of the intracluster medium (ICM) on time scales below 1 Gyr (Fabian 2012; McNamara & Nulsen 2012).

The cores of CCCs are however not completely devoid of cold gas. A study of 16 CCCs has revealed $10^9 - 10^{11.5} M_{\odot}$ of molecular gas within several tens of kiloparsecs of their BCGs (Edge 2001). Similarly, a substantial fraction of CCCs host partially ionized filamentary gas with temperature $T \sim 10^4$ K, that is emitting copious amounts of H α photons (Heckman et al. 1989; Hatch et al. 2007; McDonald et al. 2010; McDonald 2011). The H α filaments are thought to form out of marginally unstable ICM (McDonald et al. 2010; Mc-

Court et al. 2012; Sharma et al. 2012), possibly triggered by AGN feedback (Werner et al. 2014; Li & Bryan 2014; Li et al. 2015; Prasad et al. 2015; Gaspari et al. 2012, 2015; Tremblay et al. 2015; McNamara et al. 2016; Voit et al. 2017; Hogan et al. 2017). This hypothesis is supported by observations, which show a *positive* correlation between the amount of molecular gas and the jet power in early-type galaxies (Babyk et al. 2018). Along similar lines, Lakhchaura et al. (2018) find tentative evidence for a weak positive correlation between the AGN jet power and H α + [N II] luminosity in giant ellipticals.

These findings imply that the presence of cold gas necessitates AGN feedback, but do not uniquely answer the question how the cold gas is affected by it. In a recent study, based on 3D radiation-hydrodynamic simulations, we find that AGN feedback in CCCs promotes the formation of the H α filaments, and that their presence is a signpost for an ongoing or a very recent outburst of AGN feedback (Qiu et al. 2018, hereafter Q18). In this work, we examine the relationship between the properties of the H α filaments with the feedback power from SMBHs in central cluster galaxies.

2. SIMULATIONS OF AGN FEEDBACK

[†]geoyuqiu@gatech.edu

[‡]tamarab@gatech.edu

The suite of 3D radiation-hydrodynamic simulations analyzed in this work are carried out with the adaptive mesh refinement code **Enzo**+**MORAY** (Bryan et al. 2014; Wise & Abel 2011). Their key aspects are summarized below, and more detailed description of the numerical setup can be found in Q18. In this work we show results of the two representative high-resolution runs (RT02 and TI07). The main difference between them is in the modeling of radiation transport: in RT02 we calculate it explicitly using the ray-tracing module **MORAY**, while in TI07 we approximate it by injecting in the vicinity of the SMBH thermal energy commensurate to the energy of the radiation emitted by the central AGN. In all other regards the two runs are identical and produce consistent results.

The cluster is centered on a computation domain with size $(500 \text{ kpc})^3$ and modeled with maximum numerical resolution of 0.24 kpc , achieved in the cluster core. The gravitational potential of the cluster is modeled as the sum of static components: the NFW dark matter profile (Navarro et al. 1996), the BCG stellar bulge (Mathews et al. 2006), and the central SMBH (Wilman et al. 2005). The initial conditions for the ICM are based on the observed temperature and density profiles of the Perseus cluster (Churazov et al. 2004; Mathews et al. 2006; Li & Bryan 2012). The gas comprises 6 species: H I, H II, He I, He II, He III, and e^- . The radiative cooling for the H and He species utilizes the non-equilibrium cooling implemented in **Enzo**, supplemented by a cooling table to describe additional radiation losses due to metals (Smith et al. 2008). A constant value of metallicity, $Z = 0.011$, is assumed throughout the cluster.

Simulated AGN feedback is powered by accretion onto the central SMBH, such that the total feedback luminosity, $L = \eta \dot{M}_{\text{BH}} c^2$, where $\eta = 10\%$ is the feedback efficiency. The SMBH accretion rate is dominated by accretion of the cold gas ($T < 3 \times 10^4 \text{ K}$), and is estimated as $\dot{M}_{\text{BH}} \approx \epsilon_{\text{acc}} \dot{M}_{\text{cg}} / \tau$, where $\epsilon_{\text{acc}} = 10^{-3}$ is the accretion efficiency, \dot{M}_{cg} is the mass of the cold gas within the central 1 kpc , and $\tau = 5 \text{ Myr}$ is the free-fall timescale. The feedback power is allocated to the kinetic and radiative luminosity of the AGN as $L = L_K + L_R$. In this model, the AGN feedback is assumed to be radiatively inefficient when $\dot{M}_{\text{BH}} \leq 0.05 \dot{M}_{\text{Edd}}$. In this regime $L_K \propto \dot{M}_{\text{BH}}$ dominates over $L_R \propto \dot{M}_{\text{BH}}^2$. Above this accretion threshold the AGN feedback is modeled as radiatively efficient and in runs RT02 and TI07 we assume that its luminosity is equally divided between the kinetic and radiative modes, so that $L_K = L_R \propto \dot{M}_{\text{BH}}$.

3. H α FILAMENTS AS A MEASURE OF AGN FEEDBACK POWER

In this section we consider several properties of the H α filaments measured from our simulations (spatial extent, mass, and velocity dispersion) and examine their correlations with AGN feedback power. Precisely how the filaments form (i.e., whether they form in situ or are launched from the center of the cluster) will be examined in a companion paper.

3.1. Spatial Extent of the Filaments

In this section we examine whether the radial displacement of the filaments from the cluster center correlates with AGN luminosity. In order to determine the radial displacement at a given time, r_{fil} , we divide the simulated cluster into radial shells of thickness 1.7 kpc , and identify the radius of the outermost shell in which the cold gas¹ mass exceeds $10^3 M_\odot$. We have verified that other values between $10^3 - 10^7 M_\odot$ give similar results.

The left panel of Figure 1 shows the spatial extent of the filaments as a function of time from simulation TI07. The figure also shows the kinetic luminosity, associated with the AGN jets, averaged over the dynamical timescale of the filaments. This timescale is calculated as $\Delta t_{\text{fil}} = r_{\text{fil}} / v_{\text{out}}$, where $v_{\text{out}} \approx 500 \text{ km s}^{-1}$ is a characteristic outflow speed of the filaments in our simulations. For example, $\Delta t_{\text{fil}} \approx 10^8 \text{ yr}$ for filaments with $r_{\text{fil}} = 50 \text{ kpc}$. The average kinetic luminosity calculated in this way is similar to the luminosity inferred from the X-ray measurements of cavities inflated in the ICM by jets, and is different from the instantaneous kinetic luminosity determined from, for example, the radio observations. Visual inspection reveals that more powerful outbursts of AGN feedback tend to produce more spatially extended filaments.

The right panel of Figure 1 shows the kinetic luminosity as a function of the spatial extent of the filaments over the evolution of the cluster. There are two distinct trends visible in this panel. One pertains to the early time in the evolution, in the first $\sim 2 \text{ Gyr}$, when the H α filaments extend radially out in all directions from the cluster center, as illustrated in Figure 3. After 2 Gyr , the subsequent AGN outbursts result in filaments that are more collimated along the jet axis, and the jet power and the extent of the filaments can be characterized by the following correlation:

$$\langle L_K \rangle = 8.9 \times 10^{44} \text{ erg s}^{-1} \left(\frac{r_{\text{fil}}}{100 \text{ kpc}} \right)^{0.77}. \quad (1)$$

¹ In simulations, the cold gas is represented by H I. In reality, this gas phase also includes H₂, which can power intra-filament star formation.

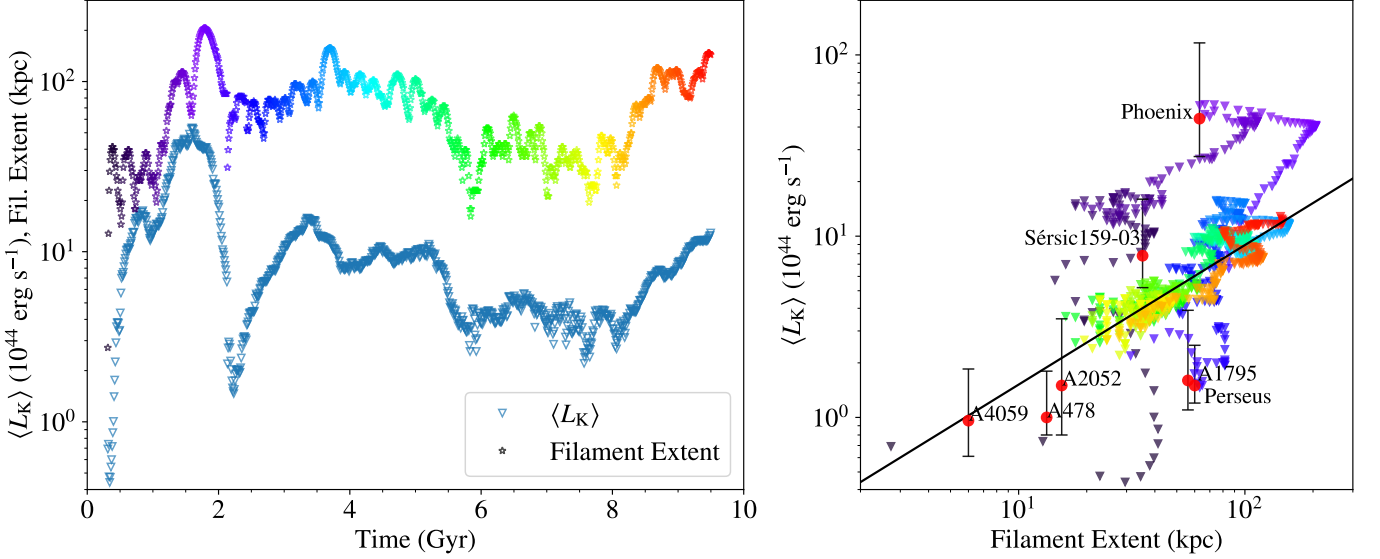


Figure 1. *Left:* Evolution of the average kinetic luminosity, $\langle L_K \rangle$ (blue triangles), and the spatial extent of the filaments (multicolor stars) measured from simulation T107. *Right:* $\langle L_K \rangle$ as a function of the filament extent. The black solid line shows the fit for data points between 2 – 9.5 Gyr. The color marks the time in the simulation. Red circles mark the observed clusters with extended H α filaments from McDonald et al. (2010, 2015). The measurements of the X-ray cavity power and associated uncertainties are from Rafferty et al. (2006) and McDonald et al. (2015).

This correlation can be understood by considering the freely expanding (or free-falling) filaments in a spherically symmetric gravitational potential, defined by the radial acceleration $g(r)$. In the absence of forces other than gravity, the terminal radius (r_f) of filaments launched with initial velocity v_i from the radius r_i is determined by the conservation of energy

$$\int_{r_i}^{r_f} g(r) dr = -\frac{1}{2} v_i^2. \quad (2)$$

Assuming that in the spatial region of interest, the acceleration can be represented by a power law, $g(r) \propto -r^\alpha$, then the specific kinetic energy at launch is $k_i = \frac{1}{2} v_i^2 \propto r_f^{\alpha+1}$ (provided that $\alpha \neq -1$). In the scenario where the initial kinetic energy of the filaments is supplied by AGN feedback, this implies $L_K \propto r_f^{\alpha+1}$. In our simulations, α is defined by the cluster potential and varies from -0.6 to -0.2 between 10 and 100 kpc (see Appendix A in Q18). For the H α filaments that extend freely to ~ 100 kpc this implies $L_K \propto r_f^{0.8}$.

This dependence closely corresponds to that shown in equation 1, measured for the evolution of filaments after the initial 2 Gyr, indicating that in this stage the filaments that form in jet-driven outflows expand freely into the ICM. This is not the case during the first 2 Gyr, when higher kinetic luminosity is required to produce the H α filaments of similar spatial extent. We find that in the initial stages of evolution the expanding filaments collide and are scattered in all directions by the infalling filaments. As a consequence, their spatial extent is sup-

pressed relative to the later stages of evolution, when the “channel” is cleared for the filaments to expand along the jet axis.

The right panel of Figure 1 also illustrates the properties of several observed clusters that host extended H α filaments (McDonald et al. 2010, 2015). The kinetic luminosity for these systems has been inferred from the size of their X-ray cavities (Rafferty et al. 2006). It is interesting to note that in the context of our simulations the Phoenix cluster corresponds to the systems in which a large amount of cold gas obstructs the expansion of the outflowing filaments. Our simulations suggest that the Perseus cluster should also be in this category, because its H α filaments extend radially out in all directions from the cluster center (Conselice et al. 2001). The implication is that about 10^8 yr ago Perseus had a powerful AGN outburst with luminosity of $\sim 10^{45}$ erg s $^{-1}$. If so, the kinetic luminosity inferred from the size of the X-ray cavities in Perseus falls short of this value by about one order of magnitude. This apparent discrepancy may be explained if the central AGN has created multiple cavities during this feedback episode, some of which could not be identified in observations.

3.2. Mass of the Filaments

In this section we investigate the degree of correlation between the AGN feedback luminosity and the mass of the H α filaments, M_{fil} . The left panel of Figure 2 shows the evolution of the average AGN luminosity (both kinetic and radiative) and M_{fil} measured from simulation

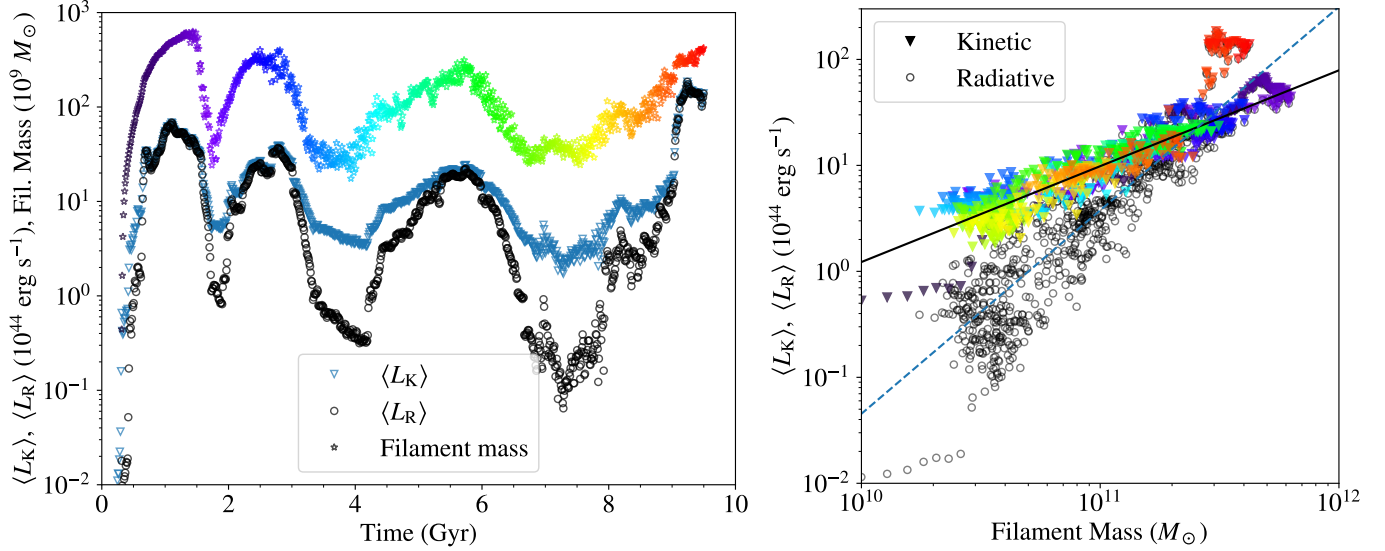


Figure 2. *Left:* Evolution of the average kinetic (blue triangles), radiative luminosity (black circles), and the H α filament mass (multicolor stars) measured in simulation RT02. *Right:* The kinetic (multicolor triangle) and radiative (black circle) luminosity as a function of the filament mass. Correlation of $\langle L_K \rangle$ ($\langle L_R \rangle$) with the H α filament mass is represented by the solid black (dashed blue) line. The color marks the time in the simulation.

RT02. $\langle L_K \rangle$ and $\langle L_R \rangle$ are averaged over the dynamical timescale of the filaments, as described in Section 3.1. We measure M_{fil} as the mass of the H I gas with rotational velocity $< 300 \text{ km s}^{-1}$. This criterion allows us to distinguish the filaments from a kinematically separate, rotationally supported cold gas disk that forms at the center of the cluster, and is visible in the middle and right panels of Figure 3.

The resulting relation between $\langle L_K \rangle$ and M_{fil} is shown in the right panel of Figure 2. In this case, a linear regression fit of the correlation yields

$$\langle L_K \rangle = 1.2 \times 10^{44} \text{ erg s}^{-1} \left(\frac{M_{\text{fil}}}{10^{10} M_\odot} \right)^{0.90}. \quad (3)$$

In the context of our model this implies $M_{\text{fil}} \propto L_K \propto \dot{M}_{\text{BH}}$. If AGN feedback in real systems operates in the same way, this suggests that the mass (or equivalently luminosity) of the H α filaments can be used as a probe of the SMBH accretion rate. Similarly, in Figure 2, the relation between the radiative AGN luminosity, $\langle L_R \rangle$, and M_{fil} can be characterized as

$$\langle L_R \rangle = 4.5 \times 10^{42} \text{ erg s}^{-1} \left(\frac{M_{\text{fil}}}{10^{10} M_\odot} \right)^{1.9}. \quad (4)$$

Following equation 3, this implies $L_R \propto M_{\text{fil}}^2 \propto \dot{M}_{\text{BH}}^2$. This relationship of L_K and L_R with the SMBH mass accretion rate is a consequence of the prescription used in our simulations to describe the allocation of the AGN luminosity between the kinetic and radiative feedback in the radiatively inefficient accretion state (see Section 2).

Thus, the correlations with M_{fil} in equations 3 and 5 apply to radiatively inefficient AGNs and they may differ for radiatively efficient AGNs.

This point is illustrated by the high luminosity outburst at the end of the simulation, represented by the red data points, which do not fall on either correlation. These data points are associated with the radiatively efficient (high luminosity) state of the SMBH, when it appears as a radio-loud quasar. Large amounts of energy injected into the ICM by jets and radiation partially suppress the formation of the H α filaments, thus shifting the data points to the left of the relation.

3.3. Velocity Distribution of the Filaments

If perturbation and turbulence associated with the AGN feedback catalyze the formation of cold gas in the ICM as hypothesized, one would then expect that AGN luminosity should also correlate with the velocity dispersion of the H α filaments. We therefore examine the relationship between the AGN feedback power and velocity distribution of H α filaments.

The top panels of Figure 3 illustrate the line-of-sight velocity (v_{los}) distribution of filaments measured from simulation RT02 corresponding to the early ($t = 0.65 \text{ Gyr}$) and late stages ($t = 3.61$ and 4.94 Gyr) in cluster evolution. As discussed in Section 3.1, the early stages are characterized by the H α filaments that extend radially out in all directions. In later stages, however, the filaments are collimated along the jet axis (here oriented along the z -axis), thereby establishing a preferential axis that breaks the spherical symmetry in the

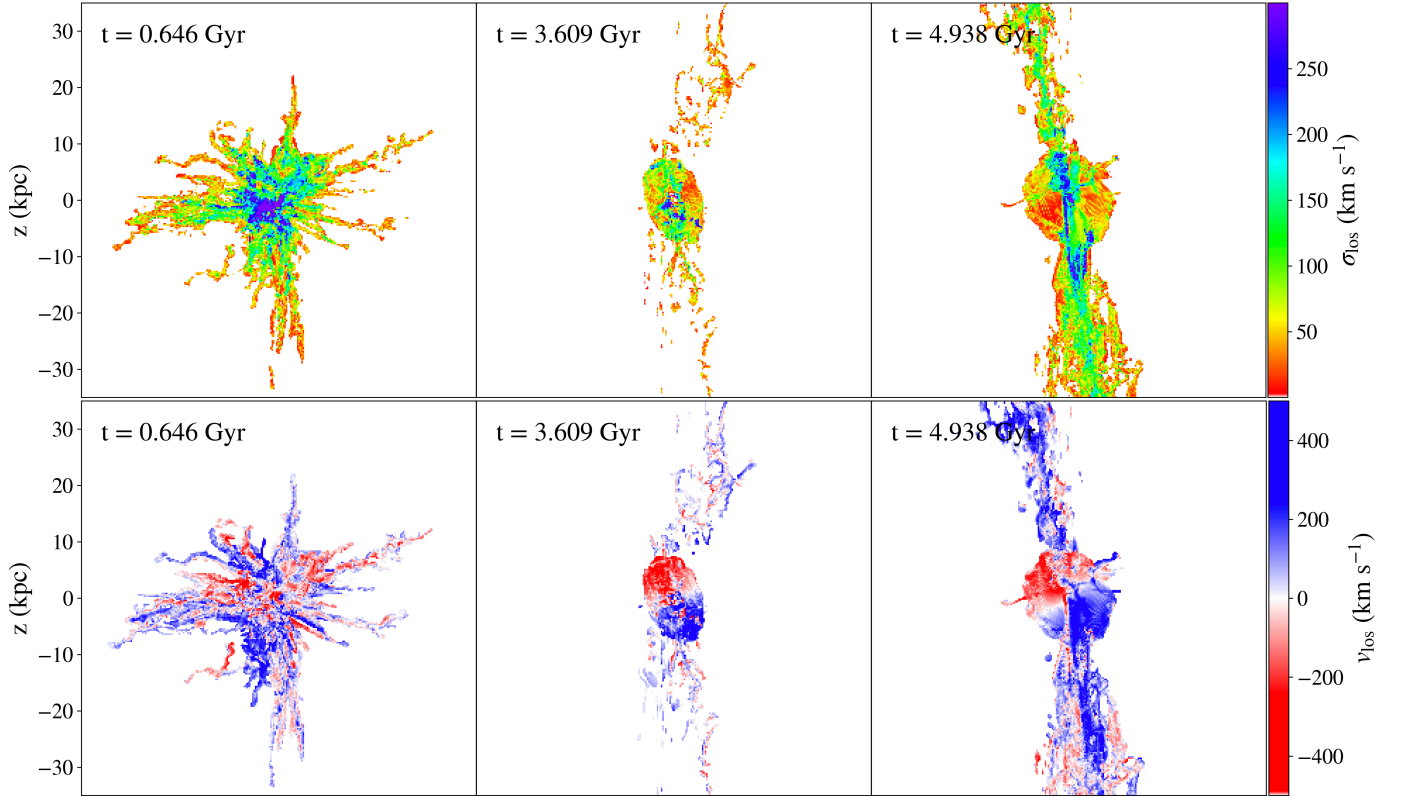


Figure 3. The line-of-sight velocity (top) and line-of-sight velocity dispersion (bottom) maps calculated for the H α filaments that are predominantly radial ($t = 0.65$ Gyr) or collimated along the jet axis ($t = 3.61$ and 4.94 Gyr) in run RT02.

velocity dispersion. The filament velocity in this image is weighted by their H α luminosity, in order to produce a map with similar properties as those obtained from observations. For this purpose, the H α luminosity of the gas is assumed to be proportional to the rate of recombination of electrons and protons, which takes the form:

$$L_{H\alpha} \propto n_p n_e T_4^{-0.942 - 0.031 \ln T_4}, \quad (5)$$

where n_p and n_e are the proton and electron number density, respectively, and $T_4 \equiv T/10^4$ K (Dong & Draine 2011; Draine 2011). This emission is in our simulations mainly contributed by the recombination of plasma with temperature $\sim 10^4$ K, and we do not account for the attenuation of the H α photons due to absorption and scattering. The resulting velocity maps have a lot of similarities with the H α filaments in Perseus and other clusters (McDonald et al. 2012; Gendron-Marsolais et al. 2018), as well as with other simulations of CCCs (Li et al. 2018; Gaspari et al. 2018).

The bottom panels of Figure 3 show the line-of-sight velocity dispersion (σ_{los}) of the filaments in the same simulation snapshots. σ_{los} is calculated in each pixel of the image as a statistical dispersion around the average velocity in each pencil beam along the line of sight, weighted by the local H α luminosity. The cross

section of each pencil beam used in this calculation is $0.25 \text{ kpc} \times 0.25 \text{ kpc}$.

In order to investigate the relationship with the AGN feedback power, we calculate the velocity dispersion of the entire network of the H α filaments in directions along and perpendicular to the jet axis. We find no statistically significant correlation of the perpendicular components with the feedback power and measure their time averaged values, $\langle \sigma_x \rangle = 161 \pm 23 \text{ km s}^{-1}$ and $\langle \sigma_y \rangle = 162 \pm 33 \text{ km s}^{-1}$, shown with the value of one standard deviation. Similarly, during the early evolution of the cluster ($t < 2$ Gyr) we find no correlation with the value of velocity dispersion along the jet axis, $\langle \sigma_z \rangle = 348 \pm 79 \text{ km s}^{-1}$. In the later stages of evolution ($2 \text{ Gyr} < t < 9 \text{ Gyr}$) however, σ_z correlates positively with the kinetic luminosity. This correlation is illustrated in Figure 4 and is characterized by the following linear regression fit

$$\langle L_K \rangle = 7.0 \times 10^{44} \text{ erg s}^{-1} \left(\frac{\sigma_z}{300 \text{ km s}^{-1}} \right)^{1.6}. \quad (6)$$

As a consequence of the assumptions in our feedback model a corresponding relation exists between $\langle L_R \rangle$ and σ_z . We do not show it here because the kinetic feedback is the primary underlying cause of the correlation. If this correlation is applicable to the real H α filament systems

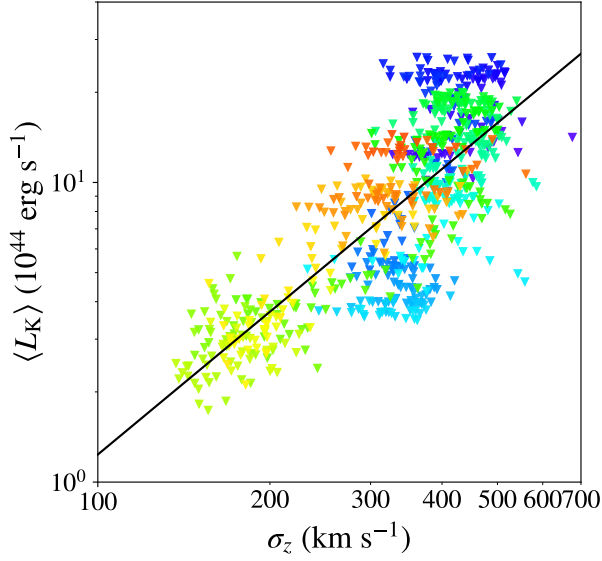


Figure 4. $\langle L_K \rangle$ as a function of the velocity dispersion of the $\text{H}\alpha$ filaments along the jet axis, σ_z . Data points correspond to $2 < t < 9$ Gyr in simulation RT02, with the same color scheme as in Figure 2. The black solid line is the linear regression fit to the data.

in observed CCCs, it implies that the measured velocity dispersion is a function of the viewing angle, and that it may be used as an independent constraint on the spatial orientation of the jet axis.

4. DISCUSSION & CONCLUSIONS

In this work we use 3D radiation-hydrodynamic simulations of AGN feedback in galaxy clusters to examine and quantify the relationship between the observable properties of the $\text{H}\alpha$ filaments and the kinetic and radiative feedback from supermassive black holes in BCGs. We summarize the main findings and simplifying assumptions below.

- We find that the AGN feedback in CCCs promotes the formation of spatially extended $\text{H}\alpha$ filaments and that their presence coincides with an ongoing outburst of AGN feedback. We identify two distinct distributions of filaments in our simulations. One is predominantly radial (similar to the Perseus cluster) and it arises when the expanding filaments collide and are scattered in all directions by the infalling filaments. The other exhibits filaments collimated along the jet axis and arises when the outflowing filaments can expand freely into the ICM.
- The spatial extent of the collimated $\text{H}\alpha$ filaments correlates with the kinetic luminosity of AGN feed-

back in such way that more luminous AGNs tend to produce more extended $\text{H}\alpha$ filament networks. This correlation can be used as a diagnostic for AGN feedback in nearby clusters, in which the extent and distribution of the filaments can be spatially resolved.

- We also report a correlation between the kinetic and radiative luminosity of AGN feedback with the mass of the $\text{H}\alpha$ filaments. The correlation implies that $M_{\text{fil}} \propto L_K \propto \dot{M}_{\text{BH}}$ and therefore the filament mass can be used to probe the AGN feedback and the rate of fueling of the central SMBH. This correlation can in principle be applied to about half of all clusters, which exhibit nuclear $\text{H}\alpha$ emission (McDonald et al. 2010), regardless of whether their filaments are spatially resolved or not.
- We find a correlation between the kinetic luminosity of AGN feedback and velocity dispersion along the jet axis (σ_z) only in the case when the filaments are collimated along the jet axis and are expanding freely into the ICM. We find no statistically significant correlation with the velocity dispersion measured perpendicular to the jet axis or with velocity dispersion of the filaments with radial distribution. If applicable to the $\text{H}\alpha$ filament systems in observed CCCs, this correlation may be used as an independent constraint on the spatial orientation of the jet axis.

Our analysis assumes that the $\text{H}\alpha$ photons are produced by the recombination of thermal plasma, aided by AGN feedback. We do not consider the effect of additional sources of ionizing radiation (like star forming regions), cosmic rays, or magnetic fields on the properties of the $\text{H}\alpha$ filaments or their emissivity. We also do not explicitly model the chemistry (i.e., the formation and destruction) of molecular gas or star formation in our simulations and are thus unable to make quantitative statements about them.

Support for this work was provided by the National Aeronautics and Space Administration through Chandra Award Number TM7-18008X issued by the Chandra X-ray Center, which is operated by the Smithsonian Astrophysical Observatory for and on behalf of the National Aeronautics Space Administration under contract NAS803060. TB acknowledges support from the National Science Foundation under grant No. NSF AST-1333360 during the early stages of this work.

REFERENCES

- Babyk, I. V., McNamara, B. R., Tamhane, P. D., et al. 2018, ArXiv e-prints. <https://arxiv.org/abs/1810.11465>
- Bryan, G. L., Norman, M. L., O’Shea, B. W., et al. 2014, *ApJS*, 211, 19, doi: 10.1088/0067-0049/211/2/19
- Churazov, E., Forman, W., Jones, C., Sunyaev, R., & Böhringer, H. 2004, *MNRAS*, 347, 29, doi: 10.1111/j.1365-2966.2004.07201.x
- Conselice, C. J., Gallagher, III, J. S., & Wyse, R. F. G. 2001, *AJ*, 122, 2281, doi: 10.1086/323534
- Dong, R., & Draine, B. T. 2011, *ApJ*, 727, 35, doi: 10.1088/0004-637X/727/1/35
- Draine, B. T. 2011, *Physics of the Interstellar and Intergalactic Medium*
- Edge, A. C. 2001, *MNRAS*, 328, 762, doi: 10.1046/j.1365-8711.2001.04802.x
- Fabian, A. C. 2012, *ARA&A*, 50, 455, doi: 10.1146/annurev-astro-081811-125521
- Gaspari, M., Brighenti, F., & Temi, P. 2015, *A&A*, 579, A62, doi: 10.1051/0004-6361/201526151
- Gaspari, M., Ruszkowski, M., & Sharma, P. 2012, *ApJ*, 746, 94, doi: 10.1088/0004-637X/746/1/94
- Gaspari, M., McDonald, M., Hamer, S. L., et al. 2018, *ApJ*, 854, 167, doi: 10.3847/1538-4357/aaa1b
- Gendron-Marsolais, M., Hlavacek-Larrondo, J., Martin, T. B., et al. 2018, *MNRAS*, doi: 10.1093/mnras/sly084
- Hatch, N. A., Crawford, C. S., & Fabian, A. C. 2007, *MNRAS*, 380, 33, doi: 10.1111/j.1365-2966.2007.12009.x
- Heckman, T. M., Baum, S. A., van Breugel, W. J. M., & McCarthy, P. 1989, *ApJ*, 338, 48, doi: 10.1086/167181
- Hogan, M. T., McNamara, B. R., Pulido, F. A., et al. 2017, *ApJ*, 851, 66, doi: 10.3847/1538-4357/aa9af3
- Lakhchaura, K., Werner, N., Sun, M., et al. 2018, ArXiv e-prints. <https://arxiv.org/abs/1806.00455>
- Li, Y., & Bryan, G. L. 2012, *ApJ*, 747, 26, doi: 10.1088/0004-637X/747/1/26
- . 2014, *ApJ*, 789, 153, doi: 10.1088/0004-637X/789/2/153
- Li, Y., Bryan, G. L., Ruszkowski, M., et al. 2015, *ApJ*, 811, 73, doi: 10.1088/0004-637X/811/2/73
- Li, Y., Ruszkowski, M., & Tremblay, G. 2018, *ApJ*, 854, 91, doi: 10.3847/1538-4357/aaa843
- Mathews, W. G., Faltenbacher, A., & Brighenti, F. 2006, *ApJ*, 638, 659, doi: 10.1086/499119
- McCourt, M., Sharma, P., Quataert, E., & Parrish, I. J. 2012, *MNRAS*, 419, 3319, doi: 10.1111/j.1365-2966.2011.19972.x
- McDonald, M. 2011, *ApJL*, 742, L35, doi: 10.1088/2041-8205/742/2/L35
- McDonald, M., Veilleux, S., & Rupke, D. S. N. 2012, *ApJ*, 746, 153, doi: 10.1088/0004-637X/746/2/153
- McDonald, M., Veilleux, S., Rupke, D. S. N., & Mushotzky, R. 2010, *ApJ*, 721, 1262, doi: 10.1088/0004-637X/721/2/1262
- McDonald, M., McNamara, B. R., van Weeren, R. J., et al. 2015, *ApJ*, 811, 111, doi: 10.1088/0004-637X/811/2/111
- McNamara, B. R., & Nulsen, P. E. J. 2012, *New Journal of Physics*, 14, 055023, doi: 10.1088/1367-2630/14/5/055023
- McNamara, B. R., Russell, H. R., Nulsen, P. E. J., et al. 2016, *ApJ*, 830, 79, doi: 10.3847/0004-637X/830/2/79
- Navarro, J. F., Frenk, C. S., & White, S. D. M. 1996, *ApJ*, 462, 563, doi: 10.1086/177173
- Prasad, D., Sharma, P., & Babul, A. 2015, *ApJ*, 811, 108, doi: 10.1088/0004-637X/811/2/108
- Qiu, Y., Bogdanovic, T., Li, Y., Park, K., & Wise, J. H. 2018, ArXiv e-prints. <https://arxiv.org/abs/1810.01857>
- Rafferty, D. A., McNamara, B. R., Nulsen, P. E. J., & Wise, M. W. 2006, *ApJ*, 652, 216, doi: 10.1086/507672
- Sharma, P., McCourt, M., Quataert, E., & Parrish, I. J. 2012, *MNRAS*, 420, 3174, doi: 10.1111/j.1365-2966.2011.20246.x
- Smith, B., Sigurdsson, S., & Abel, T. 2008, *MNRAS*, 385, 1443, doi: 10.1111/j.1365-2966.2008.12922.x
- Tremblay, G. R., O’Dea, C. P., Baum, S. A., et al. 2015, *MNRAS*, 451, 3768, doi: 10.1093/mnras/stv1151
- Voit, G. M., Meece, G., Li, Y., et al. 2017, *ApJ*, 845, 80, doi: 10.3847/1538-4357/aa7d04
- Werner, N., Oonk, J. B. R., Sun, M., et al. 2014, *MNRAS*, 439, 2291, doi: 10.1093/mnras/stu006
- Wilman, R. J., Edge, A. C., & Johnstone, R. M. 2005, *MNRAS*, 359, 755, doi: 10.1111/j.1365-2966.2005.08956.x
- Wise, J. H., & Abel, T. 2011, *MNRAS*, 414, 3458, doi: 10.1111/j.1365-2966.2011.18646.x